INORGANIC CHEMISTRY
FRONTIERS

RESEARCH ARTICLE

View Article Online
View Journal | View Issue

Check for updates

Cite this: *Inorg. Chem. Front.*, 2024, **11**, 6577

Enhancers of amyloid aggregation: novel ferrocene-based compounds selective toward amyloid models†

Sara La Manna,*[a] Concetta Di Natale,[b] Valeria Panzetta,[b,c] Paolo Antonio Netti,[b,c] Antonello Merlino,[d] Konrad Kowalski[e] and Daniela Marasco*[a]

Amyloid aggregation is at the molecular basis of neurodegeneration and provides toxic species which trigger the progression of the disease. Hence, there is an urgent need to identify novel molecules able to suppress toxicity either through an inhibitory or enhancing effect on aggregation. Herein, the effects of two metal complexes bearing a ferrocene unit and one or two propen-thyminyl groups, namely **mono-T_Fc** and **di-T_Fc**, on the aggregation properties of two different amyloid models were investigated. In detail, the peptide spanning residues 264–277 of the protein nucleophosmin 1 and that covering the C-terminal tail of the Aβ peptide ($A\beta_{21-40}$) were chosen as amyloidogenic systems with different primary sequences and mechanisms of self-aggregation. UV–vis absorption spectroscopy, thioflavin T fluorescence assay and autofluorescence techniques were employed to evaluate the stability of **mono-T_Fc** and **di-T_Fc** and the effects of their presence on the aggregation of the investigated amyloidogenic peptides. The compounds selectively enhance the self-recognition of $A\beta_{21-40}$ with a more marked effect exhibited by **di-T_Fc**, which contains two thymines. Scanning electron microscopy, dynamic light scattering and preliminary cell viability assays performed in SHSY5 cells confirm this result, which is due to the formation of metal-compound/peptide adducts as assessed by electrospray ionization mass spectrometry.

Received 24th July 2024,
Accepted 10th August 2024

DOI: 10.1039/d4qi01854k

rsc.li/frontiers-inorganic

Open Access Article. Published on 15 August 2024. Downloaded on 2/13/2026 6:11:47 AM.
This article is licensed under a Creative Commons Attribution-NonCommercial 3.0 Unported Licence.

Introduction

Amyloidogenesis is the major process underlying neuronal damage and memory impairment in Alzheimer's disease (AD) and other neurodegenerative disorders (NDDs).[1,2] It involves the production and accumulation of amyloid plaques due to the self-aggregation of amyloid-β (Aβ) peptides to form soluble oligomers, protofibrils and insoluble fibrils.[3] Aggregation is a molecular phenomenon regulated by many experimental factors such as pH values[4] and concentration levels of metal ions.[5,6] Aggregation occurs through the self-recognition of peptides or protein monomers in misfolded/unfolded states.[7] The modulation of the Aβ aggregation process is therefore considered an effective therapy for preventing neuronal damage and cognitive decline.

However, the translation of potential drugs from *in vitro* studies into effective treatments *in vivo* has proven challenging.[8] This difficulty often stems from a lack of comprehensive understanding of the multiple mechanisms involved in Aβ aggregation and the complexity of the *in vivo* environment.[9]

The therapeutic regulation of amyloid aggregation may concern: (i) the inhibition of aggregation limiting the formation of toxic species[10] or (ii) acceleration of aggregation to induce the formation of large oligomers which are less toxic species.[11] Indeed, there is an inverse correlation between the size and the toxicity of amyloid oligomers: smaller oligomers

[a]*Department of Pharmacy, University of Naples Federico II, 80131 Naples, Italy. E-mail: sara.lamanna@unina.it, daniela.marasco@unina.it*
[b]*Department of Ingegneria Chimica del Materiali e della Produzione Industriale (DICMAPI), University of Naples Federico II, 80125 Naples, Italy*
[c]*Interdisciplinary Research Centre on Biomaterials (CRIB), University of Naples Federico II, Istituto Italiano di Tecnologia, 80125 Naples, Italy*
[d]*Department of Chemical Sciences, University of Naples Federico II, 80126 Naples, Italy*
[e]*University of Łódź, Faculty of Chemistry, Department of Organic Chemistry, Tamka 12, 91-403 Łódź, Poland*

†Electronic supplementary information (ESI) available: Fig. S1: UV-vis spectra over time of **mono-T_Fc** and **di-T_Fc** and solubility assays; Fig. S2: overlay of fluorescence emission spectra normalized for the concentrations of compounds; Fig. S3: overlay of the fluorescence emission spectra of **mono-T_Fc** and **di-T_Fc**; Fig. S4: raw correlation with DLS of $A\beta_{21-40}$ alone and with **mono-T_Fc** after 4 and 6 h of aggregation Fig. S5: ESI-MS spectra of **mono-T_Fc** and **di-T_Fc**; Fig. S6: SEM micrographs of **mono-T_Fc** and **di-T_Fc**; Fig. S7: SEM micrographs of Aβ21-40 in the absence and presence of **mono-T_Fc** or **di-T_Fc**; Fig. S8: SEM micrographs of NPM1264–277 in the absence and presence of **mono-T_Fc** or **di-T_Fc**; Table S1: $t_{\frac{1}{2}}$ and maximum −+ values related to ThT experiments; Table S2: table of the main observed ions relative to the species formed by $A\beta_{21-40}$ alone and mixed with **di-T_Fc** or **mono-T_Fc**; Table S3: table of the main observed ions relative to the species formed by the $NPM1_{264-277}$ peptide alone and mixed with **di-T_Fc** or **mono-T_Fc**. See DOI: https://doi.org/10.1039/d4qi01854k

Open Access Article. Published on 15 August 2024. Downloaded on 2/13/2026 6:11:47 AM.
This article is licensed under a Creative Commons Attribution-NonCommercial 3.0 Unported Licence.

tend to exhibit greater toxicity compared to larger oligomers or fibrils.[12] Hundreds of studies have been carried out to design and identify external agents such as organic compounds of synthetic[13] and natural origins (*e.g.* anthracyclines,[14] tetracyclines,[15] sterols,[16] polyphenols,[17] epigallocatechin gallate, resveratrol and curcumin[18]), peptides,[19] antibodies[20] and metallodrugs[21–28] mainly as inhibitors or, more in general, modulators[29] of toxic aggregation cascades by preventing or dissolving the pre-formed aggregates that determine structural changes during self-recognition. The failure of many inhibitors in clinical trials for NDDs highlights the need to better understand the complex interactions that occur during plaque formation, including binding to carbohydrates, lipids, nucleic acids, and metal ions.[30] Unravelling how modulators interact with Aβ peptides, for example, and how they change their aggregation process may provide opportunities for the development of new therapies,[31] since the modulation of fibrillar growth may regulate the final size and shape of non-covalent assemblies, thereby altering the cellular properties of aggregates.[32] Recently, the enhancement of amyloid aggregation has become a promising strategy to modulate the Aβ aggregation process;[33–35] accelerating agents are often endowed with multifunctional groups able to target multiple regions of Aβ peptides and able to speed up aggregation, as demonstrated by polyethyleneimine–perphenazine conjugates.[36] Several natural compounds have shown enhancing effects on Aβ peptide aggregation, as glycosaminoglycans, which are able to reduce the cellular toxicity of $A\beta_{25-35}$ [37] and $A\beta_{1-42}$ [38] through the acceleration of fibril formation, as well as polyphosphate, which can act as a universal accelerator of amyloid aggregation of curli fibers, α-synuclein, $A\beta_{1-40/42}$ and Tau subunits.[39] Other accelerators stabilize the formation of aggregates: trodusquemine is able to stabilize $A\beta_{1-42}$ aggregates,[40] orcein derivatives stabilize human islet amyloid polypeptide (hIAPP) aggregates,[41,42] and small aromatic compounds, resulting from the screening of a library of PPI inhibitors, selectively stabilize hIAPP aggregates but not those of $A\beta_{1-42}$.[43]

Among the potential neurodrugs, metallodrugs have received particular attention[44] especially recently[45,46] due to their unique properties, which depend on the metal and the nature of metal ligands.[47] An important strategy in inorganic medicinal chemistry is the incorporation of bioactive molecules as ligands, including clinically approved drugs, in a repurposing approach to overcome drug resistance and to design promising alternatives to currently available metal-based drugs.[48,49]

Recently, a remarkable renaissance of interest in the complexes of transition metal ions with pyrimidine nucleobases has occurred.[50,51] Herein, we investigated the ability to act as modulators of aggregation of two metal complexes which belong to a burgeoning class of organometallic/nucleic acid conjugates.[52]

In detail, ferrocenyl–nucleobase conjugates can combine the hydrophobicity of the ferrocenyl moiety with hydrogen-bonding capabilities of the nucleobase moiety[53,54] and, as far as we know, this is the first report on this class of compounds as amyloid aggregation modulators. These complexes, named **mono-T_Fc** and **di-T_Fc** (Fig. 1), contain a ferrocene unit and one or two propen-thyminyl groups, respectively, as substituents on the cyclopentadienyl rings.[55] Indeed, biologically active ferrocenyl compounds are derived from the conjugation of ferrocene with biologically relevant molecules.[56] The synthesis of **mono-T_Fc** and **di-T_Fc** compounds was already reported.[55,57]

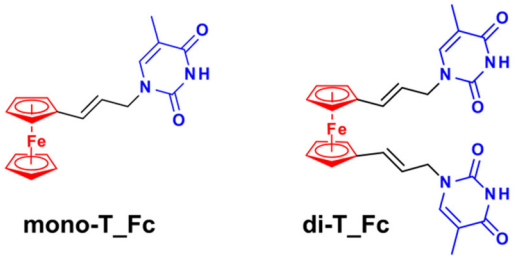

Peptide	Sequence	pI
$NPM1_{264-277}$	VEAKFINYVKNCFR	10.15
$A\beta_{21-40}$	AEDVGSNKGAIIGLMVGGVV	6.98

Fig. 1 Chemical structures of the ferrocene-based compounds **mono-T_Fc** and **di-T_Fc** with the ferrocenyl group in red and thymine in blue and sequences and theoretical isoelectric points (pIs) of the amyloid peptide models investigated in this study.

An interesting approach for the screening of Aβ aggregation modulators is to use protein/peptide amyloids that, although not strictly involved in neurodegeneration, are considered structural models of amyloids.[58–60] Nucleophosmin 1 (NPM1) is not a neurodegenerative protein but it contains, in the second helix of its C-terminal domain (CTD), a well-characterized fragment, spanning residues 264–277 ($NPM1_{264-277}$),[61] which has been already used as an amyloid model[23,62] Conversely, we also employed as amyloid model the fragment spanning residues 21–40 of the Aβ polypeptide, $A\beta_{21-40}$, which covers the C-terminal region of $A\beta_{1-42}$ and is directly involved in its aggregation process.[26]

In this study, the effects of metal compounds **mono-T_Fc** and **di-T_Fc** on the aggregation propensity of $A\beta_{21-40}$ and $NPM1_{264-277}$ peptides were investigated. Thioflavin T (ThT) fluorescence assay, time-dependent autofluorescence, dynamic light scattering (DLS) and scanning electron microscopy (SEM) were employed. The direct interactions between $A\beta_{21-40}$ and $NPM1_{264-277}$ and the metal compounds were assessed by electrospray ionization mass spectrometry (ESI-MS) studies. Their cellular effects on the toxicity of amyloids were tested in SHSY5 cells.

Results and discussion

Effects of metal complexes on the kinetics of aggregation of $A\beta_{21-40}$ and $NPM1_{264-277}$ ThT assays

Prior to evaluating their specific effects on amyloid aggregation, the stability of the metal complexes in aqueous buffer was evaluated by monitoring their UV-vis absorption spectral profiles at different times and concentrations (Fig. S1,† upper panel). Both complexes, at 25 μM, are stable over 4 hours,

This journal is © the Partner Organisations 2024

Open Access Article. Published on 15 August 2024. Downloaded on 2/13/2026 6:11:47 AM. This article is licensed under a Creative Commons Attribution-NonCommercial 3.0 Unported Licence.

showing overlapping absorption spectra (Fig. S1A and B†). At 75 μM, a slight reduction in the absorbance is observed, especially in the case of **di-T_Fc**, which seems less stable than **mono-T_Fc** (Fig. S1D†). To assess whether this difference was due to different water solubilities of the compounds, the concentration dependence of absorbance was evaluated. Interestingly, the metal complexes show different behaviors: the concentration dependence of absorbance is linear for **mono-T_Fc** in the 25–100 μM range (Fig. S1E†), while it is limited to the 12.5–50 μM concentration range in the case of **di-T_Fc** (Fig. S1F†). To gain insights into this behavior, fluorescence spectra were recorded for both compounds and the overlays of emission spectra normalized with respect to the concentrations of the compounds are presented in Fig. S2.† The emission spectra are superimposable only at two initial concentrations (10 and 25 μM), while at higher concentrations, above all 75 μM, a quenching effect, likely due to stacking interactions, is observable.

Once the concentrations of the compounds that can be used for the subsequent analyses are established, the effects of the presence of **mono-T_Fc** and **di-T_Fc** on the aggregation kinetics of $A\beta_{21-40}$ and $NPM1_{264-277}$ were evaluated using the ThT fluorescence assay (Fig. 2).

Time course profiles indicate different effects of the metal compounds on amyloidogenic peptide aggregation and to properly compare them, $t\frac{1}{2}$ and fluorescence maxima values are also reported in Table S1.† The presence of both complexes has a clear enhancing effect on the aggregation of $A\beta_{21-40}$, which is more marked for **di-T_Fc** than for **mono-T_Fc** (Fig. 2A and C). The initial values of ThT signals, in the absence and presence of complexes, were almost superimposable (Fig. 2A) and in agreement with those already reported.[23,62] Interestingly, the effect of the presence of **di-T_Fc** (Fig. 2C) on the aggregation of $A\beta_{21-40}$, depends on the peptide : complex molar ratio (Table S1†). At a peptide : complex molar ratio of 1 : 0.5, a greater increase in the ThT signal is detected compared to the 1 : 1 and 1 : 1.5 ratios with maxima at 3768.7, 2342.5 and 1278.6 a.u., respectively. This could be due to the presence of two propen-thyminyl units in the structure of **di-T_Fc**, which could anchor $A\beta_{21-40}$ in different points, favouring its self-assembly. Conversely, at higher concentrations of **di-T_Fc**, 50 and 75 μM, for 1 : 1 and 1 : 1.5 ratios, respectively, stacking interactions among the complex molecules prevail, providing a lower active concentration. Indeed, from Fig. 2C, it is evident that in the presence of amyloid $A\beta_{21-40}$, stacking prevails at lower concentrations with respect to those determined in the absence of peptides (see Fig. S1F†), suggesting that the hydrophobic character of the peptide could prompt stacking phenomena in the case of **di-T_Fc**. At a ratio of 1 : 0.2, there is no appreciable effect because of the very low amount of **di-T_Fc** when compared to $A\beta_{21-40}$. Notably, the presence of **di-T_Fc** and **mono-T_Fc** during $NPM1_{264-277}$ aggregation causes only a slight reduction of the ThT signal, suggesting a poor inhibitory effect (Fig. 2B and D).

To gain insights into the enhancing effects of **mono-T_Fc** and **di-T_Fc** on $A\beta_{21-40}$ aggregation, an amyloid seeding assay

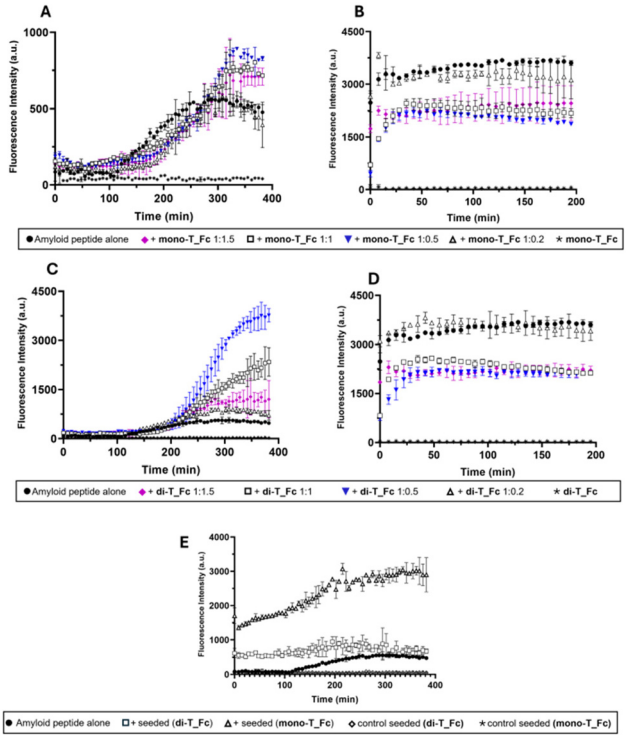

Fig. 2 Overlay of time-courses of ThT fluorescence emission intensity at 482 nm of $A\beta_{21-40}$ (A and C) and $NPM1_{264-277}$ (B and D) in the presence or absence of **mono-T_Fc** (A and B) and **di-T_Fc** (C and D) at indicated peptide : metal complex molar ratios. (E) Amyloid seeding assay (ASA) of $A\beta_{21-40}$ with the seed $A\beta_{21-40}$+ metal complex at a 1 : 0.5 molar ratio. The results are representatives of two independent experiments.

(ASA) was carried out (Fig. 2E). In this experiment, $A\beta_{21-40}$ pre-aggregated with **di-T_Fc** or **mono-T_Fc** (in a peptide to complex molar ratio of 1 : 0.5) acts as a seed for the aggregation of freshly prepared $A\beta_{21-40}$, leading to an increase in fluorescence intensity already at $t = 0$. The fluorescence profile of $A\beta_{21-40}$ treated with seeds with **mono-T_Fc** shows a significant increase in intensity, reaching a maximum value of 3043 a.u. (Table S1†). This suggests the formation of soluble oligomers of higher dimensions than those found in the absence of seeds. A similar experiment in the presence of seeds formed with **di-T_Fc** shows a plateau already at 200 min and a reduction of the $t_{1/2}$ value of approximately 45 min with respect to the value of the peptide alone and a subsequent slight decrease of intensity, probably due to the formation of insoluble fibrils that tend to precipitate. To gain insights into the observed different behaviours of the Fc complexes toward the amyloids, the lipophilicity of the complexes was assessed by calculating their $\log P$ values using the classical flask method.[63] Both complexes showed $\log P$ values above 0 (0.82 for **mono-T_Fc** and 0.23 for **di-T_Fc**), suggesting a marked hydrophobic character. This finding could explain the observed preference of the complexes to interact with the nearly neutral sequence of $A\beta_{21-40}$ rather than that of $NPM1_{264-277}$.

Open Access Article. Published on 15 August 2024. Downloaded on 2/13/2026 6:11:47 AM.
This article is licensed under a Creative Commons Attribution-NonCommercial 3.0 Unported Licence.

Effects of metal complexes on the amyloid aggregates: autofluorescence and DLS assays

In the last twenty years, many studies have pointed out the onset of a novel intrinsic autofluorescence, which is strictly related to the fibrillization process. Indeed, upon excitation in the UV range (280–400 nm), numerous amyloid systems exhibit autofluorescence properties, characterised by an emission in the visible range (400–490 nm). This spectral feature is often called "deep-blue autofluorescence".[64]

We analysed the effects of the presence of **mono-T_Fc** and **di-T_Fc** on the autofluorescence properties of the amyloid models[23,62] by monitoring emission spectra upon excitation at 440 nm over time (Fig. 3). $A\beta_{21-40}$ alone exhibits an increase in emission intensities at λ = 477 and 515 nm over time (Fig. 3A). In the presence of **di-T_Fc**, a progressive shift toward higher wavelengths (481 nm) and a related intensity increase, with a concomitant disappearance of the band centered at 515 nm, were observed (Fig. 3C). In the presence of **mono-T_Fc**, a slight increase in fluorescence intensity (Fig. 3B) was found. The same analysis carried out for $NPM1_{264-277}$ confirms the poor ability of the complexes to modulate $NPM1_{264-277}$ aggregation; indeed, no appreciable variations are visible in the spectra recorded in the presence of the complexes when compared to those recorded with the peptide alone (Fig. 3D–F). Control experiments reveal a negligible fluorescence of the two compounds upon excitation at 440 nm (Fig. S3†).

Then the DLS technique was employed to evaluate the effects of the complexes on the aggregate size (Fig. 4). The samples of peptides in the absence and presence of the complexes (peptide : metal complex molar ratio of 1 : 0.5) were monitored overtime. Correct autocorrelation was achieved only for the sample formed using $A\beta_{21-40}$ and **di-T_Fc**, after 4 h under stirring. In this case the $A\beta_{21-40}$ aggregates with a diameter of ~1555 nm (Fig. 4). The formation of these large aggregates confirms the role of **di-T_Fc** as an enhancer agent of Aβ peptide aggregation. Under the same conditions, metal-free $A\beta_{21-40}$ in the presence **mono-T_Fc** did not provide autocorrelation (Fig. S4†).

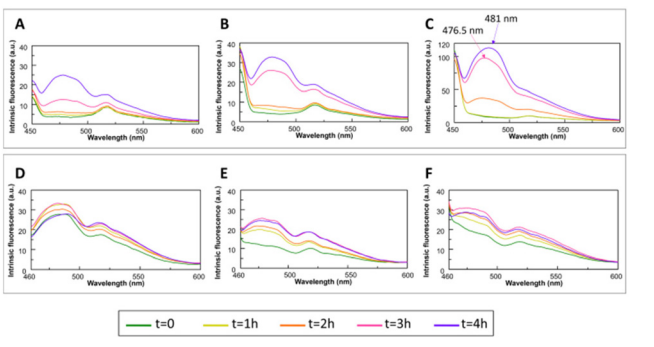

Fig. 3 Overlay of the fluorescence emission spectra of $A\beta_{21-40}$ (upper panel) and $NPM1_{264-277}$ (lower panel) in the absence (A and D) and presence of **mono-T_Fc** (B and E) and **di-T_Fc** (C and F) at different times (λ_{ex} = 440 nm and 1 : 0.5 peptide : complex molar ratio).

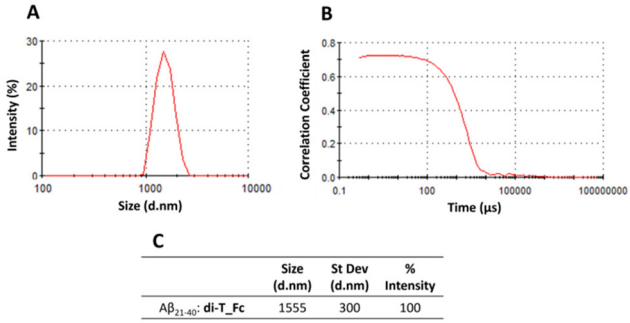

C

	Size (d.nm)	St Dev (d.nm)	% Intensity
$A\beta_{21-40}$: **di-T_Fc**	1555	300	100

Fig. 4 Size distribution (A) and raw correlation (B) by DLS of $A\beta_{21-40}$ with **di-T_Fc** at a 1 : 0.5 peptide : metal complex molar ratio recorded after 4 h of aggregation. (C) Dynamic parameters of DLS analysis.

The low limit of detection of the oligomers obtained by DLS strictly depends on the nature of the sample (usually 80–100 nm in size),[65] thus the lack of autocorrelation in the case of $A\beta_{21-40}$ alone and in the presence of **mono-T_Fc** indicates that for both complexes the size of the oligomers is under this limit.

ESI-MS analysis of adducts between the complexes and $NPM1_{264-277}$ and $A\beta_{21-40}$

To evaluate a possible direct interaction between the peptides and the two metal complexes, we employed native electrospray ionization mass spectrometry (ESI-MS).

For this purpose, $NPM1_{264-277}$ or $A\beta_{21-40}$ peptides were incubated with the metal compounds (at a 1 : 0.5 peptide to metal complex molar ratio) and the samples were analyzed at t = 0 of aggregation (Fig. 5 and 6). The peptides and complexes alone were analyzed as references (Fig. 5, 6 and S5†) and the peaks recorded are summarized in Tables S2 and 3.† In the case of $A\beta_{21-40}$ (Fig. 5A), signals of the b-series were generated from spontaneous in-source fragmentation events, as previously reported.[66] In the presence of **mono-T_Fc** (Fig. 5B), two additional peaks at m/z 1118.68 and 746.7 a.m.u. were found.

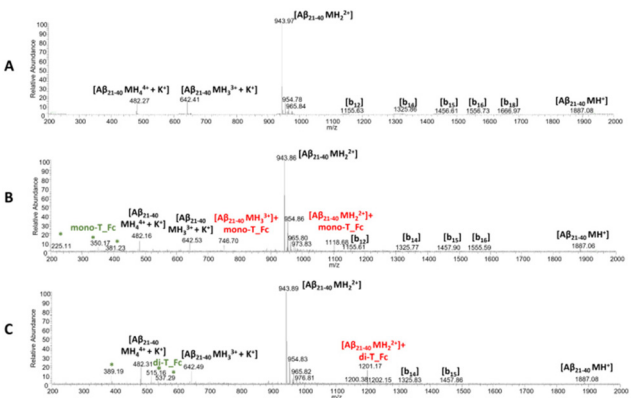

Fig. 5 ESI-MS spectra of $A\beta_{21-40}$ in the absence (A) and presence of **mono-T_Fc** (B) and **di-T_Fc** (C). The asterisks highlight the species that are present also in the MS spectra of the complexes alone (Fig. S5†).

This journal is © the Partner Organisations 2024

Open Access Article. Published on 15 August 2024. Downloaded on 2/13/2026 6:11:47 AM.
This article is licensed under a Creative Commons Attribution-NonCommercial 3.0 Unported Licence.

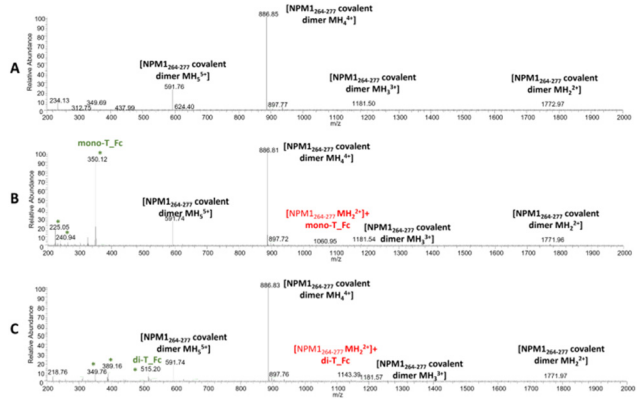

Fig. 6 ESI-MS spectra of $NPM1_{264-277}$ in the absence (A) and presence of **mono-T_Fc** (B) and **di-T_Fc** (C). The asterisks highlight the species that are present also in the MS spectra of the complexes alone.

These peaks are assigned to $A\beta_{21-40}$ with one **mono-T_Fc** molecule. In the presence of **di-T_Fc** (Fig. 5C), a peak at *m*/*z* 1201.17 a.m.u., related to $A\beta_{21-40}$ with one **di-T_Fc** molecule was observed. However, in this case, fewer peaks than those found for **mono-T_Fc**, due to in source fragmentation, were found. These results can be due to the formation of larger adducts (see the DLS results) which are likely unable to correctly ionize.[23]

Similar experiments were carried out for $NPM1_{264-277}$; related ESI-MS spectra are presented in Fig. 6. Peaks at *m*/*z* 1772.9, 1181.50, 886.85 and 591.76 a.m.u. are due the presence of a disulfide-bridged dimer and these peaks persist in the presence of metal complexes, even if peaks attributed to the peptide with one molecule of **mono-T_Fc** and **di-T_Fc**, respectively, are observed (Fig. 6 and Table S3†).

Effects of metal complexes on the morphologies of amyloid fibers

The effects of **mono-T_Fc** and **di-T_Fc** on the morphologies of $NPM1_{264-277}$ and $A\beta_{21-40}$ aggregates were investigated through SEM. All samples were obtained and analyzed after mixing at a 1 : 0.5 peptide : complex molar ratio. After 4 h of aggregation, the $A\beta_{21-40}$ speptide alone provides long mature fibers with an average length of ~1000 μm and a diameter of ~50 μm (Fig. 7A and Table 1).[66] In the presence of metal complexes, these fibers are more structured with increased values of length and diameter (Fig. 7B, C and Table 1), in line with already reported data for amyloid enhancer agents.[23,67] Also, $NPM1_{264-277}$ alone shows long well-defined fibers with a length of ~1000 μm and a diameter of ~30 μm (Fig. 7D and Table 1). For this peptide, the presence of metal compounds does not determine an increase in fiber size, indeed the fibers observed in the presence of **mono-T_Fc** are rather similar to those of $NPM1_{264-277}$ (Fig. 7F), while those found in the presence of **di-T_Fc** are shorter and thinner than those of the peptide alone (Fig. 7E and Table 1). As expected, the complexes alone do not form fibers under the investigated experimental conditions (Fig. S6†).

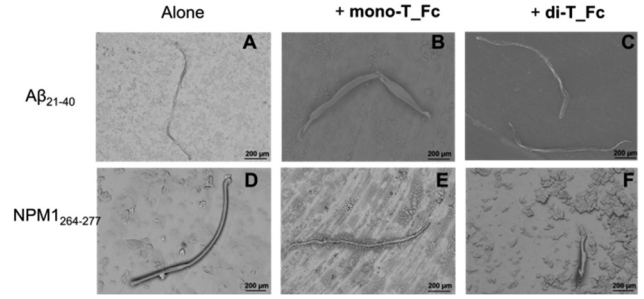

Fig. 7 SEM micrographs of $A\beta_{21-40}$ (A–C) and $NPM1_{264-277}$ (D–F) in the absence and presence of **mono-T_Fc** or **di-T_Fc** at a 1 : 0.5 peptide : metal complex molar ratio.

Table 1 SEM analyses. Average diameters and lengths of the fibers obtained for $A\beta_{21-40}$ and $NPM1_{264-277}$ (see Fig. S7 and S8†) in the presence and absence of **mono-T_Fc** and **di-T_Fc** determined using the software ImageJ[68]

	Average diameter (μm) ×10	Average length (μm) ×10^3
$A\beta_{21-40}$	4.7 ± 0.3	1.0 ± 0.8
$A\beta_{21-40}$ + **mono-T_Fc**	7.4 ± 0.8	1.8 ± 0.9
$A\beta_{21-40}$ + **di-T_Fc**	6.0 ± 0.2	1.9 ± 0.9
$NPM1_{264-277}$	2.6 ± 0.1	1.0 ± 0.9
$NPM1_{264-277}$ + **mono-T_Fc**	3.0 ± 0.1	1.4 ± 1.0
$NPM1_{264-277}$ + **di-T_Fc**	3.4 ± 0.1	0.40 ± 0.08

Cellular effects of metal complexes on the amyloid cytotoxicity of $A\beta_{21-40}$

As a preliminary step, the effects of the metal complexes on the cytotoxicity of $A\beta_{21-40}$ on SHSY5Y cells were analyzed using the MTT assay (Fig. 8).

As expected, $A\beta_{21-40}$ reduces the cell viability of ~15% only at t = 4 h, while the presence of **di-T_Fc** with the Aβ peptide induces toxicity already at t = 0, not comparable to that of the

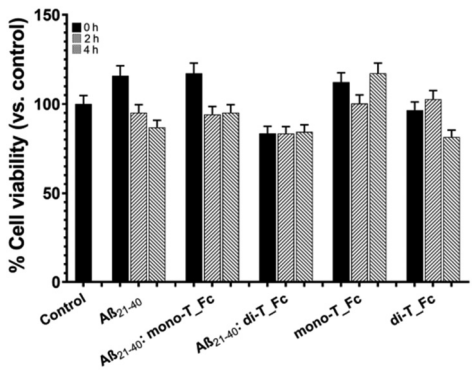

Fig. 8 Cytotoxic effect of molecules on SHSY5Y cells: MTT assay of $A\beta_{21-40}$ in the absence and presence of **mono-T_Fc** and **di-T_Fc** incubated under stirring at t = 0, 2 and 4 h. We refer to the control untreated cells (control) as 100% of viable cells. Statistical analysis was calculated using GraphPad Prism 9 by two-way ANOVA with Šídák's multiple comparison test.

Open Access Article. Published on 15 August 2024. Downloaded on 2/13/2026 6:11:47 AM. This article is licensed under a Creative Commons Attribution-NonCommercial 3.0 Unported Licence.

di-T_Fc complex alone. This toxicity is presumably due to the formation of high-order oligomers and remains almost constant for 4 h of aggregation, suggesting the progression of oligomerization, as also indicated by DLS experiments. $A\beta_{21-40}$ with **mono-T_Fc** exhibited a behavior more similar to that of the peptide alone.

Experimental

Synthesis of metal compounds and peptides

$A\beta_{21-40}$ and $NPM1_{264-277}$ were synthesized as previously reported.[69] After purification, peptides were treated with 1,1,1,3,3,3-hexafluoro-2-propanol (HFIP) and then stored at −20 °C until use. The synthesis of **mono-T_Fc** and **di-T_Fc** was already reported.[38,55] **Mono-T_Fc** exhibited a 0.022 V *vs.* FcH/FcH + redox couple.[38]

Determination of log *P*

The logarithmic partition coefficient log *P* between 1-octanol and water phases was determined for both complexes using the shake flask method. The complexes were dissolved in an equal volume of water (pre-saturated with 1-octanol) and 1-octanol (pre-saturated with ultrapure water) to achieve a final concentration of 25 μM. The mixtures were shaken mechanically for 120 min at 25 °C and then centrifuged to assist with bilayer formation. The experiments were performed at least in duplicate.

The concentrations in the water phase were determined by UV-vis absorption (BioDrop DUO spectrophotometer) employing for **mono-T_Fc** $\varepsilon_{275\ nm}$ = 8500 cm^{-1} M^{-1} bearing one propen-thymine and for **di-T_Fc** $\varepsilon_{275\ nm}$ = 17 000 cm^{-1} M^{-1} bearing two propen-thymine groups.[70] The log *P* was calculated according to the following equation by assuming $C_{octanol} = C_{total} - C_{water}$ (*C*: complex concentration):

$$\log P = \log \frac{C_{octanol}}{C_{water}}.$$

UV-vis absorption spectroscopy

The solution stability of **mono-T_Fc** and **di-T_Fc** was evaluated by obtaining their UV-vis absorption spectra in 10 mM phosphate buffer at pH 7.4 for 24 hours. To obtain the UV-vis absorption spectra, the compounds were dissolved in DMSO (50 mM stock solution) and then added to the selected buffers to achieve a final concentration of 25 or 75 μM. The final concentration of DMSO was 0.2% (v/v). UV-vis absorption spectra were recorded on BioDrop Duo UV Visible Spectrophotometers (Cambridge, United Kingdom) at room temperature using 1 cm path length cuvettes and the following parameters: 290–600 nm range, 200 nm min^{-1}, and 2.0 nm bandwidth.

Fluorescence spectroscopy

To evaluate stacking effects, emission spectra of **di-T_Fc** and **mono-T_Fc** were recorded in a 10 × 2 mm path-length cuvette using λ_{exc} = 260 nm and λ_{em} range: 270–600 nm. Assays were performed at 25 °C in 50 mM phosphate buffer at pH 7.4 at concentrations of 10, 25, 50 and 75 μM. Spectra were normalized as the fluorescence intensity divided by the complex concentration.

ThT emission assay was carried out using an Envision 2105 fluorescence reader (PerkinElmer) in black plates (96 well) under stirring. Measurements were performed every 2 min (λ_{exc}: 440 nm and λ_{em}: 485 nm). Assays were performed at 25 °C employing a peptide concentration of 50 μM in 50 mM phosphate buffer at pH 7.4 using a ThT final concentration of 50 μM at different molar ratios with metal complexes (50 mM stock solution in DMSO, final DMSO concentration 0.2%). Amyloid seeding assays (ASAs) were performed employing $A\beta_{21-40}$ (50 μM) pre-aggregated with **di-T_Fc** or **mono-T_Fc** at a 1 : 0.5 peptide : metal complex molar ratio for 4 hours in 50 mM phosphate buffer at pH 7.4. The seeded samples were added to the $A\beta_{21-40}$ monomer (50 μM) at a final concentration of 5 μM, providing a seed : monomer molar ratio of 1 : 10. As controls, the seeded samples were added to 50 mM phosphate buffer at pH 7.4.

Autofluorescence experiments were carried out on a JASCO FP 8300 spectrofluorometer, in a 10 × 2 mm path-length cuvette using a peptide concentration of 50 μM in 50 mM phosphate buffer at pH 7.4 in the absence or presence of complexes at a 1 : 0.5 peptide : metal compound molar ratio; λ_{exc}: 440 nm and λ_{em} range: 450–600 nm.

ESI-MS analysis

The solution of $A\beta_{21-40}$ or $NPM1_{264-277}$ at a concentration of 50 μM in 15 mM ammonium acetate (AMAC)[71,72] buffer at pH = 7.0 was incubated with **di-T_Fc** or **mono-T_Fc** in a peptide to metal compound molar ratio of 1 : 0.5. The solutions were diluted 10 times with 15 mM AMAC and then analyzed using a LTQ XL ion trap mass spectrometer equipped with an electrospray ionization (ESI) source operating at a needle voltage of 3.5 kV and 320 °C with a complete Ultimate 3000 HPLC system, including a pump MS, an autosampler, and a photodiode array (all from Thermo Fisher Scientific). Spectra of the isolated peptides and the two complexes alone were recorded as controls.

DLS assays

DLS measurements were performed using a Zetasizer Nano S DLS device from Malvern Instruments (Malvern, Worcestershire, UK) with a 633 nm laser, a backscatter angle of 173°, thermostated with a Peltier system and a plastic micro-cuvette. $A\beta_{21-40}$ with a concentration of 50 μM in 50 mM phosphate buffer at pH 7.4 and 25 °C alone or at a 1 : 0.5 peptide to metal complex molar ratio was kept under stirring. Size distributions by intensity were determined in automatic mode at regular time-intervals over a period of 10 min for each measurement. Thirteen acquisitions were recorded, each of 10 seconds in duration.

Scanning electron microscopy

SEM micrographs were taken using the SEM-Hitachi TM3000 configuration and preparation protocols as previously

 This journal is © the Partner Organisations 2024

Open Access Article. Published on 15 August 2024. Downloaded on 2/13/2026 6:11:47 AM. This article is licensed under a Creative Commons Attribution-NonCommercial 3.0 Unported Licence.

reported.[73] Briefly, samples (50 μL) 1 containing $A\beta_{21-40}$ or $NPM1_{264-277}$ (50 μM) alone or mixed with complexes at a 1 : 0.5 peptide : metal compound molar ratio (10 mM phosphate buffer at pH 7.4, final DMSO concentration 0.2%) after 4 h of stirring were mounted on microscope stubs, dried overnight, and sputter coated with gold of about 5 nm thickness.

Cell culture

The human SH-SY5Y cell line was grown under a humidified atmosphere of 5% CO_2 (37 °C) in Dulbecco's modified Eagle's medium and Ham's F12 (DMEM/F-12) containing 10% fetal bovine serum (FBS), 100 μg mL^{-1} of L-glutamine, and 100 U mL^{-1} of penicillin/streptomycin.

MTT assay

The cells were seeded in triplicate in 96-well plates at a density of 35 000 cells per well. $A\beta_{21-40}$ (200 μM stock solution in 50 mM phosphate buffer at pH 7.4) in the absence and presence of the metal complexes at a 1 : 0.5 peptide to metal complexes molar ratio (after 0, 2 and 4 h of stirring) were diluted in the cell culture medium at a final concentration of 50 μM and added to the cells and left for 24 h at 37 °C under a humidified atmosphere of 5% CO_2. The control cells were incubated with phosphate buffer diluted in the cell culture medium at the same final concentration used for the Aβ peptide. After the incubation, 200 μL of 3-(4,5-dimethylthiazol-2-yl)-2,5-diphenyltetrazolium bromide (final concentration of 0.5 mg mL^{-1} in complete cell media without red phenol; Sigma-Aldrich) was added to each well for 3 h. Isopropanol was then added to allow the reduction of MTT into formazan crystals by living cells. The optical density of each well sample was determined at 570 nm using a microplate reader. A blank absorbance value of 0.13, obtained from the wells without the cells but treated with the MTT reagent, was subtracted from all the absorbance values. Then, the average absorbance value of cells incubated with the Aβ peptide was normalized to those of control cells incubated with buffer, and the cell viability was expressed as a percentage of the control.

Conclusion

In NDDs, amyloid aggregates cause neurotoxicity through different mechanisms including the disruption of membranes, interference with electrophysiological signaling, and/or metal ion homeostasis. Hence, there is an urgent need to revert the toxicity of amyloid aggregates using chemical agents as metallodrugs. Few studies report on enhancer agents and the experimental consequences of the increase of amyloid formation such as accelerated kinetics, enlargement of oligomers[74,75] and reduced toxic effects.[67] In the present study, we have investigated the effects of two ferrocene neutral metal complexes, **mono-T_Fc** and **di-T_Fc**, containing one and two propen-thymines as ligands, respectively, on the self-aggregation of two amyloid peptide models, $A\beta_{21-40}$ and $NPM1_{264-277}$, which are endowed with different pI values, slightly acidic and very basic, respectively (Fig. 1). The two metal complexes have different effects on the aggregation of the two model systems; indeed, a neat amyloid enhancer outcome was observed in the case of $A\beta_{21-40}$, while a slight inhibition was detected in the case of $NPM1_{264-277}$. The observed selectivity toward amyloid systems is an important novelty for the employment of metallodrugs[21–28] and is likely due to both electrostatic and steric factors. Indeed, the nearly neutral state of $A\beta_{21-40}$ could favour the interaction with neutral complexes differently from $NPM1_{264-277}$. This latter sequence drives its self-aggregation mechanism mainly through aromatic interactions.[76,77] These differences could explain the opposite observed effects of the metal complexes toward self-recognition of the peptides; in the case of $A\beta_{21-40}$, the insertion of **di-T_Fc** and **mono-T_Fc** into the growing oligomers takes place without disrupting the occurring interactions, as instead observed in the case of $NPM1_{264-277}$. This enhancing effect was greater for **di-T_Fc**, which bears two propen-thyminyl moieties. The presence of a nucleobase is crucial in this enhancing mechanism, in agreement with the results obtained using cymantrene-containing complexes coordinated to adenine.[23] The enhancer effect is so high for **di-T_Fc** that micrometric $A\beta_{21-40}$ oligomers are observed for the first time. Nevertheless, the narrowed water solubility and active concentration ranges of **di-T_Fc** represent limiting factors in its direct translation as a selective neurodrug.

Overall, this study strongly supports the hypothesis that ferrocene/nucleic acid conjugates are selective modulators of different amyloids and can be considered as a future class of therapeutic agents at early stages of amylogenesis. Future molecular modeling investigations could unveil structural determinants of recognition between amyloids with known structural features and thymine–Fc complexes and could aid the design of analogues through the introduction of appropriate chemical modifications to enhance their water solubility and specificity and modulate their enhancing/inhibitor effects.

Author contributions

S. L. M. synthesized the peptides and performed fluorescence, UV and DLS studies; K. K. provided the samples of complexes reported previously from his lab, discussed the obtained results and helped in manuscript preparation; C. D. N. performed SEM analysis; V. P. and P. A. N. performed cellular experiments; D. M., A. M., K. K. and S. L. M. designed the concept and supervised the experiments; D. M., A. M., K. K. and S. L. M. wrote the manuscript. All authors have read and approved the final version of the manuscript.

Data availability

The data supporting this article have been included as part of the ESI.†

Open Access Article. Published on 15 August 2024. Downloaded on 2/13/2026 6:11:47 AM. This article is licensed under a Creative Commons Attribution-NonCommercial 3.0 Unported Licence.

Conflicts of interest

There are no conflicts to declare.

Acknowledgements

This work was supported by #NEXTGENERATIONEU (NGEU), the Ministry of University and Research (MUR), National Recovery and Resilience Plan (NRRP), project MNESYS (PE0000006) – a multiscale integrated approach to the study of the nervous system in health and disease (DN. 1553 11.10.2022) and partially by Associazione Italiana per la Ricerca sul Cancro (AIRC) grant IG 2022, Rif. 27378 (D. M.).

References

1 D. Ghosh, S. Samanta and T. Govindaraju, Dihydrophthalazinediones accelerate amyloid β peptide aggregation to nontoxic species, *Bull. Mater. Sci.*, 2020, **43**, 1–8.
2 A.-H. Emwas, M. Alghrably, M. Dhahri, A. Sharfalddin, R. Alsiary, M. Jaremko, G. Faa, M. Campagna, T. Congiu and M. Piras, Living with the enemy: From protein-misfolding pathologies we know, to those we want to know, *Ageing Res. Rev.*, 2021, **70**, 101391.
3 F. Chiti and C. M. Dobson, Protein misfolding, amyloid formation, and human disease: a summary of progress over the last decade, *Annu. Rev. Biochem.*, 2017, **86**, 27–68.
4 C. M. Duarte, Ł. Jaremko and M. Jaremko, Hypothesis: potentially systemic impacts of elevated CO2 on the human proteome and health, *Front. Public Health*, 2020, **8**, 543322.
5 B. G. Poulson, K. Szczepski, J. I. Lachowicz, L. Jaremko, A.-H. Emwas and M. Jaremko, Aggregation of biologically important peptides and proteins: inhibition or acceleration depending on protein and metal ion concentrations, *RSC Adv.*, 2020, **10**, 215–227.
6 M. Alghrably, D. Dudek, A.-H. Emwas, Ł. Jaremko, M. Jaremko and M. Rowińska-Żyrek, Copper(II) and amylin analogues: A complicated relationship, *Inorg. Chem.*, 2020, **59**, 2527–2535.
7 G. Wei, Z. Su, N. P. Reynolds, P. Arosio, I. W. Hamley, E. Gazit and R. Mezzenga, Self-assembling peptide and protein amyloids: from structure to tailored function in nanotechnology, *Chem. Soc. Rev.*, 2017, **46**, 4661–4708.
8 B. Decourt, K. Noorda, K. Noorda, J. Shi and M. N. Sabbagh, Review of Advanced Drug Trials Focusing on the Reduction of Brain Beta-Amyloid to Prevent and Treat Dementia, *J. Exp. Pharmacol.*, 2022, **14**, 331–352.
9 J. Han, Z. Du and M. H. Lim, Mechanistic insight into the design of chemical tools to control multiple pathogenic features in Alzheimer's disease, *Acc. Chem. Res.*, 2021, **54**, 3930–3940.
10 Q. Wang, X. Yu, L. Li and J. Zheng, Inhibition of amyloid-beta aggregation in Alzheimer's disease, *Curr. Pharm. Des.*, 2014, **20**, 1223–1243.
11 Y. Zhang, D. Zhang, Y. Tang, B. Ren, F. Liu, L. Xu, Y. Chang and J. Zheng, Aromadendrin: a dual amyloid promoter to accelerate fibrillization and reduce cytotoxicity of both amyloid-β and hIAPP, *Mater. Adv.*, 2020, **1**, 1241–1252.
12 U. Sengupta, A. N. Nilson and R. Kayed, The role of amyloid-β oligomers in toxicity, propagation, and immunotherapy, *EBioMedicine*, 2016, **6**, 42–49.
13 S. Oasa, V. L. Kouznetsova, I. F. Tsigelny and L. Terenius, Small molecular decoys in Alzheimer's disease, *Neural Regener. Res.*, 2024, **19**, 1658–1659.
14 G. Merlini, E. Ascari, N. Amboldi, V. Bellotti, E. Arbustini, V. Perfetti, M. Ferrari, I. Zorzoli, M. G. Marinone and P. Garini, Interaction of the anthracycline 4′-iodo-4′-deoxydoxorubicin with amyloid fibrils: inhibition of amyloidogenesis, *Proc. Natl. Acad. Sci. U. S. A.*, 1995, **92**, 2959–2963.
15 G. Forloni, L. Colombo, L. Girola, F. Tagliavini and M. Salmona, Anti-amyloidogenic activity of tetracyclines: studies in vitro, *FEBS Lett.*, 2001, **487**, 404–407.
16 I. Cook and T. S. Leyh, Sterol-activated amyloid beta fibril formation, *J. Biol. Chem.*, 2023, **299**, 105445.
17 M. Dhahri, M. Alghrably, H. A. Mohammed, S. L. Badshah, N. Noreen, F. Mouffouk, S. Rayyan, K. A. Qureshi, D. Mahmood and J. I. Lachowicz, Natural polysaccharides as preventive and therapeutic horizon for neurodegenerative diseases, *Pharmaceutics*, 2021, **14**, 1.
18 S. Giorgetti, C. Greco, P. Tortora and F. A. Aprile, Targeting amyloid aggregation: an overview of strategies and mechanisms, *Int. J. Mol. Sci.*, 2018, **19**, 2677.
19 Y. Zhang, L. A. Borch, N. H. Fischer and M. Meldal, Hydrodynamic Control of Alzheimer Aβ Fibrillation with Glucosaminic Acid Containing Click-Cyclized β-Bodies, *J. Am. Chem. Soc.*, 2023, **146**, 2654–2662.
20 E. A. Çulcu, Ş. Demiryürek and A. T. Demiryürek, Recent treatment approaches for Alzheimer's disease with monoclonal antibodies targeting amyloid-β, *Recent Trends Pharmacol.*, 2023, **1**, 150–166.
21 H. Y. Khan, A. Ahmad, M. N. Hassan, Y. H. Khan, F. Arjmand and R. H. Khan, Advances of metallodrug-amyloid β aggregation inhibitors for therapeutic intervention in neurodegenerative diseases: Evaluation of their mechanistic insights and neurotoxicity, *Coord. Chem. Rev.*, 2024, **501**, 215580.
22 S. La Manna, M. Leone, I. Iacobucci, A. Annuziata, C. Di Natale, E. Lagreca, A. M. Malfitano, F. Ruffo, A. Merlino and M. Monti, Glucosyl platinum(II) complexes inhibit aggregation of the C-terminal region of the Aβ peptide, *Inorg. Chem.*, 2022, **61**, 3540–3552.
23 S. La Manna, V. Roviello, F. Napolitano, A. M. Malfitano, V. Monaco, A. Merlino, M. Monti, K. Kowalski, L. Szczupak and D. Marasco, Metal-Complexes Bearing Releasable CO Differently Modulate Amyloid Aggregation, *Inorg. Chem.*, 2023, **62**, 10470–10480.
24 S. La Manna, C. Di Natale, V. Panzetta, M. Leone, F. A. Mercurio, I. Cipollone, M. Monti, P. A. Netti, G. Ferraro and A. Terán, A Diruthenium Metallodrug as a

 This journal is © the Partner Organisations 2024

Open Access Article. Published on 15 August 2024. Downloaded on 2/13/2026 6:11:47 AM. This article is licensed under a Creative Commons Attribution-NonCommercial 3.0 Unported Licence.

Potent Inhibitor of Amyloid-β Aggregation: Synergism of Mechanisms of Action, *Inorg. Chem.*, 2023, **63**, 564–575.

25 D. Florio, M. Cuomo, I. Iacobucci, G. Ferraro, A. M. Mansour, M. Monti, A. Merlino and D. Marasco, Modulation of Amyloidogenic Peptide Aggregation by Photoactivatable CO-Releasing Ruthenium(II) Complexes, *Pharmaceuticals*, 2020, **13**, 171.

26 D. Florio, I. Iacobucci, G. Ferraro, A. M. Mansour, G. Morelli, M. Monti, A. Merlino and D. Marasco, Role of the Metal Center in the Modulation of the Aggregation Process of Amyloid Model Systems by Square Planar Complexes Bearing 2-(2′-pyridyl)benzimidazole Ligands, *Pharmaceuticals*, 2019, **12**, 154.

27 D. Florio, S. La Manna, A. Annunziata, I. Iacobucci, V. Monaco, C. Di Natale, V. Mollo, F. Ruffo, M. Monti and D. Marasco, Ruthenium complexes bearing glucosyl ligands are able to inhibit the amyloid aggregation of short histidine-peptides, *Dalton Trans.*, 2023, **52**, 8549–8557.

28 D. Florio, A. M. Malfitano, S. Di Somma, C. Mügge, W. Weigand, G. Ferraro, I. Iacobucci, M. Monti, G. Morelli and A. Merlino, Platinum(II) O, S complexes inhibit the aggregation of amyloid model systems, *Int. J. Mol. Sci.*, 2019, **20**, 829.

29 L. Breydo and V. N. Uversky, Role of metal ions in aggregation of intrinsically disordered proteins in neurodegenerative diseases, *Metallomics*, 2011, **3**, 1163–1180.

30 K. G. Yiannopoulou, A. I. Anastasiou, V. Zachariou and S. H. Pelidou, Reasons for Failed Trials of Disease-Modifying Treatments for Alzheimer Disease and Their Contribution in Recent Research, *Biomedicines*, 2019, **7**, 97.

31 K. L. Stewart and S. E. Radford, Amyloid plaques beyond Aβ: a survey of the diverse modulators of amyloid aggregation, *Biophys. Rev.*, 2017, **9**, 405–419.

32 L. Zhu, Y. Song, P.-N. Cheng and J. S. Moore, Molecular design for dual modulation effect of amyloid protein aggregation, *J. Am. Chem. Soc.*, 2015, **137**, 8062–8068.

33 J. Bieschke, M. Herbst, T. Wiglenda, R. P. Friedrich, A. Boeddrich, F. Schiele, D. Kleckers, J. M. Lopez del Amo, B. A. Grüning and Q. Wang, Small-molecule conversion of toxic oligomers to nontoxic β-sheet–rich amyloid fibrils, *Nat. Chem. Biol.*, 2012, **8**, 93–101.

34 M. Holubová, V. Lobaz, L. Loukotová, M. Rabyk, J. Hromádková, O. Trhlíková, Z. Pechrová, O. Groborz, P. Štěpánek and M. Hrubý, Does polysaccharide glycogen behave as a promoter of amyloid fibril formation at physiologically relevant concentrations?, *Soft Matter*, 2021, **17**, 1628–1641.

35 Y. Tang, D. Zhang, X. Gong and J. Zheng, Cross-seeding enables repurposing of aurein antimicrobial peptides as a promoter of human islet amyloid polypeptide (hIAPP), *J. Mater. Chem. B*, 2023, **11**, 7920–7932.

36 P.-N. Cheng, R. Spencer, R. J. Woods, C. G. Glabe and J. S. Nowick, Heterodivalent linked macrocyclic β-sheets with enhanced activity against Aβ aggregation: two sites are better than one, *J. Am. Chem. Soc.*, 2012, **134**, 14179–14184.

37 M. Walzer, S. Lorens, M. Hejna, J. Fareed, I. Hanin, U. Cornelli and J. M. Lee, Low molecular weight glycosaminoglycan blockade of β-amyloid induced neuropathology, *Eur. J. Pharmacol.*, 2002, **445**, 211–220.

38 X. Fernàndez-Busquets, J. Ponce, R. Bravo, M. Arimon, T. Martianez, A. Gella, J. Cladera and N. Durany, Modulation of amyloid β peptide1–42 cytotoxicity and aggregation in vitro by glucose and chondroitin sulfate, *Curr. Alzheimer Res.*, 2010, **7**, 428–438.

39 C. M. Cremers, D. Knoefler, S. Gates, N. Martin, J.-U. Dahl, J. Lempart, L. Xie, M. R. Chapman, V. Galvan and D. R. Southworth, Polyphosphate: a conserved modifier of amyloidogenic processes, *Mol. Cell*, 2016, **63**, 768–780.

40 R. Limbocker, S. Chia, F. S. Ruggeri, M. Perni, R. Cascella, G. T. Heller, G. Meisl, B. Mannini, J. Habchi and T. C. Michaels, Trodusquemine enhances Aβ42 aggregation but suppresses its toxicity by displacing oligomers from cell membranes, *Nat. Commun.*, 2019, **10**, 225.

41 Y. Zou, Z. Qian, Y. Sun, G. Wei and Q. Zhang, Orcein-related small molecule O4 destabilizes hIAPP protofibrils by interacting mostly with the amyloidogenic core region, *J. Phys. Chem. B*, 2017, **121**, 9203–9212.

42 D. Florio, V. Roviello, S. La Manna, F. Napolitano, A. M. Malfitano and D. Marasco, Small molecules enhancers of amyloid aggregation of C-terminal domain of Nucleophosmin 1 in acute myeloid leukemia, *Bioorg. Chem.*, 2022, **127**, 106001.

43 Y. Xu, R. Maya-Martinez, N. Guthertz, G. R. Heath, I. W. Manfield, A. L. Breeze, F. Sobott, R. Foster and S. E. Radford, Tuning the rate of aggregation of hIAPP into amyloid using small-molecule modulators of assembly, *Nat. Commun.*, 2022, **13**, 1040.

44 K. J. Barnham, V. B. Kenche, G. D. Ciccotosto, D. P. Smith, D. J. Tew, X. Liu, K. Perez, G. A. Cranston, T. J. Johanssen and I. Volitakis, Platinum-based inhibitors of amyloid-β as therapeutic agents for Alzheimer's disease, *Proc. Natl. Acad. Sci. U. S. A.*, 2008, **105**, 6813–6818.

45 J.-M. Suh, G. Kim, J. Kang and M. H. Lim, Strategies employing transition metal complexes to modulate amyloid-β aggregation, *Inorg. Chem.*, 2018, **58**, 8–17.

46 J.-M. Suh, M. Kim, J. Yoo, J. Han, C. Paulina and M. H. Lim, Intercommunication between metal ions and amyloidogenic peptides or proteins in protein misfolding disorders, *Coord. Chem. Rev.*, 2023, **478**, 214978.

47 H. Liu, Y. Qu and X. Wang, Amyloid β-targeted metal complexes for potential applications in Alzheimer's disease, *Future Med. Chem.*, 2018, **10**, 679–701.

48 C. Sumithaa and M. Ganeshpandian, Half-Sandwich Ruthenium Arene Complexes Bearing Clinically Approved Drugs as Ligands: The Importance of Metal–Drug Synergism in Metallodrug Design, *Mol. Pharm.*, 2023, **20**, 1453–1479.

49 A. Monney and M. Albrecht, Transition metal bioconjugates with an organometallic link between the metal and the biomolecular scaffold, *Coord. Chem. Rev.*, 2013, **257**, 2420–2433.

Open Access Article. Published on 15 August 2024. Downloaded on 2/13/2026 6:11:47 AM. This article is licensed under a Creative Commons Attribution-NonCommercial 3.0 Unported Licence.

50 B. Lippert and P. J. Sanz Miguel, The renaissance of metal–pyrimidine nucleobase coordination chemistry, *Acc. Chem. Res.*, 2016, **49**, 1537–1545.
51 C. Riccardi, D. Capasso, A. Coppola, C. Platella, D. Montesarchio, S. Di Gaetano, G. N. Roviello and D. Musumeci, Synthesis, antiproliferative activity, and DNA binding studies of nucleoamino acid-containing Pt(II) complexes, *Pharmaceuticals*, 2020, **13**, 284.
52 M. Maschke, J. Grohmann, C. Nierhaus, M. Lieb and N. Metzler-Nolte, Peptide Bioconjugates of Electron–Poor Metallocenes: Synthesis, Characterization, and Anti–Proliferative Activity, *ChemBioChem*, 2015, **16**, 1333–1342.
53 K. Kowalski, Ferrocenyl-nucleobase complexes: Synthesis, chemistry and applications, *Coord. Chem. Rev.*, 2016, **317**, 132–156.
54 K. Kowalski, Organometallic nucleosides—Synthesis, transformations, and applications, *Coord. Chem. Rev.*, 2021, **432**, 213705.
55 K. Kowalski, J. Skiba, L. Oehninger, I. Ott, J. Solecka, A. Rajnisz and B. Therrien, Metallocene-modified uracils: Synthesis, structure, and biological activity, *Organometallics*, 2013, **32**, 5766–5773.
56 H. Song, X. Li, Y. Long, G. Schatte and H.-B. Kraatz, Ferrocene-modified pyrimidine nucleosides: synthesis, structure and electrochemistry, *Dalton Trans.*, 2006, 4696–4701.
57 M. Gil-Moles, S. Türck, U. Basu, A. Pettenuzzo, S. Bhattacharya, A. Rajan, X. Ma, R. Büssing, J. Wölker and H. Burmeister, Metallodrug Profiling against SARS–CoV–2 Target Proteins Identifies Highly Potent Inhibitors of the S/ACE2 interaction and the Papain–like Protease PLpro, *Chem. – Eur. J.*, 2021, **27**, 17928–17940.
58 B. Ahmad, M. S. Borana and A. P. Chaudhary, Understanding curcumin-induced modulation of protein aggregation, *Int. J. Biol. Macromol.*, 2017, **100**, 89–96.
59 V. Kovalska, S. Chernii, V. Cherepanov, M. Losytskyy, V. Chernii, O. Varzatskii, A. Naumovets and S. Yarmoluk, The impact of binding of macrocyclic metal complexes on amyloid fibrillization of insulin and lysozyme, *J. Mol. Recognit.*, 2017, **30**, e2622.
60 X. Huo, H. Liu, S. Wang, S. Yin and Z. Yin, The inhibitory effect and mechanism of small molecules on acetic anhydride-induced BSA acetylation and aggregation, *Colloids Surf., B*, 2023, **225**, 113265.
61 C. Di Natale, P. L. Scognamiglio, R. Cascella, C. Cecchi, A. Russo, M. Leone, A. Penco, A. Relini, L. Federici, A. Di Matteo, F. Chiti, L. Vitagliano and D. Marasco, Nucleophosmin contains amyloidogenic regions that are able to form toxic aggregates under physiological conditions, *FASEB J.*, 2015, **29**, 3689–3701.
62 S. La Manna, C. Di Natale, V. Panzetta, M. Leone, F. A. Mercurio, I. Cipollone, M. Monti, P. A. Netti, G. Ferraro, A. Teran, A. E. Sanchez-Pelaez, S. Herrero, A. Merlino and D. Marasco, A Diruthenium Metallodrug as a Potent Inhibitor of Amyloid-beta Aggregation: Synergism of Mechanisms of Action, *Inorg. Chem.*, 2024, **63**, 564–575.
63 A. Andrés, M. Rosés, C. Ràfols, E. Bosch, S. Espinosa, V. Segarra and J. M. Huerta, Setup and validation of shake-flask procedures for the determination of partition coefficients (log D) from low drug amounts, *Eur. J. Pharm. Sci.*, 2015, **76**, 181–191.
64 J. Mignon, T. Leyder, D. Mottet, V. N. Uversky and C. Michaux, In-depth investigation of the effect of pH on the autofluorescence properties of DPF3b and DPF3a amyloid fibrils, *Spectrochim. Acta, Part A*, 2024, **313**, 124156.
65 A. M. Streets, Y. Sourigues, R. R. Kopito, R. Melki and S. R. Quake, Simultaneous measurement of amyloid fibril formation by dynamic light scattering and fluorescence reveals complex aggregation kinetics, *PLoS One*, 2013, **8**, e54541.
66 S. La Manna, D. Florio, I. Iacobucci, F. Napolitano, I. Benedictis, A. M. Malfitano, M. Monti, M. Ravera, E. Gabano and D. Marasco, A Comparative Study of the Effects of Platinum(II) Complexes on beta-Amyloid Aggregation: Potential Neurodrug Applications, *Int. J. Mol. Sci.*, 2021, **22**, 3015.
67 P. Huettemann, P. Mahadevan, J. Lempart, E. Tse, B. Dehury, B. F. Edwards, D. R. Southworth, B. R. Sahoo and U. Jakob, Amyloid Accelerator Polyphosphate Implicated as the Mystery Density in α-Synuclein Fibrils, *bioRxiv*, 2024, preprint, DOI: **10.1101/2024.05.01.592011**.
68 C. A. Schneider, W. S. Rasband and K. W. Eliceiri, NIH Image to ImageJ: 25 years of image analysis, *Nat. Methods*, 2012, **9**, 671–675.
69 S. La Manna, V. Roviello, V. Monaco, J. A. Platts, M. Monti, E. Gabano, M. Ravera and D. Marasco, The inhibitory effects of platinum(II) complexes on amyloid aggregation: a theoretical and experimental approach, *Dalton Trans.*, 2023, **52**, 12677–12685.
70 A. Nikolaev and S. Paston, Solvent type influence on thymidine UV-sensitivity, *J. Phys.: Conf. Ser.*, 2015, **661**, 012019.
71 L. Konermann, Addressing a common misconception: ammonium acetate as neutral pH "buffer" for native electrospray mass spectrometry, *J. Am. Soc. Mass Spectrom.*, 2017, **28**, 1827–1835.
72 L. Konermann, Z. Liu, Y. Haidar, M. J. Willans and N. A. Bainbridge, On the chemistry of aqueous ammonium acetate droplets during native electrospray ionization mass spectrometry, *Anal. Chem.*, 2023, **95**, 13957–13966.
73 C. Di Natale, S. La Manna, A. M. Malfitano, S. Di Somma, D. Florio, P. L. Scognamiglio, E. Novellino, P. A. Netti and D. Marasco, Structural insights into amyloid structures of the C-terminal region of nucleophosmin 1 in type A mutation of acute myeloid leukemia, *Biochim. Biophys. Acta, Proteins Proteomics*, 2019, **1867**, 637–644.
74 J. R. Kim and R. M. Murphy, Mechanism of accelerated assembly of β-amyloid filaments into fibrils by KLVFFK6, *Biophys. J.*, 2004, **86**, 3194–3203.
75 A. M. Isaacs, D. B. Senn, M. Yuan, J. P. Shine and B. A. Yankner, Acceleration of amyloid β-peptide aggregation by physiological concentrations of calcium, *J. Biol. Chem.*, 2006, **281**, 27916–27923.

 This journal is © the Partner Organisations 2024

Open Access Article. Published on 15 August 2024. Downloaded on 2/13/2026 6:11:47 AM.
This article is licensed under a Creative Commons Attribution-NonCommercial 3.0 Unported Licence.

76 S. La Manna, D. Florio, V. Panzetta, V. Roviello, P. A. Netti, C. Di Natale and D. Marasco, Hydrogelation tunability of bioinspired short peptides, *Soft Matter*, 2022, **18**, 8418–8426.

77 D. Florio, C. Di Natale, P. L. Scognamiglio, M. Leone, S. La Manna, S. Di Somma, P. A. Netti, A. M. Malfitano and D. Marasco, Self-assembly of bio-inspired heterochiral peptides, *Bioorg. Chem.*, 2021, **114**, 105047.